

---

# Combination treatment with migrastatic inhibitors to target brain tumour spread

**Hayley Butler**

*University of Huddersfield, Queensgate, Huddersfield, West Yorkshire, HD1 3DH*

---

## ARTICLE INFO

---

*Article history:*

Received 18 October 2020

Received in revised form 12

February 2021

Accepted 06 April 2021

---

*Keywords:*

Glioblastoma Multiforme

Brain Tumour

CCG-1423

Rhosin hydrochloride

Migration

Cancer

## ABSTRACT

---

A Glioblastoma Multiforme (GBM), a malignant brain tumour, ranks highly among the most aggressive cancers. This study explored the effects of the anti-migratory drugs, CCG-1423 and Rhosin hydrochloride, on the motility of cancerous cells. Scratch wound and tumour spheroid assays were conducted on untreated and treated U87 glioma cells to observe the extent of migration. The migratory cells from the assays were fixed with paraformaldehyde to assess the expression levels and distribution of actin and focal adhesions with confocal imaging. CCG-1423 and Rhosin hydrochloride used in combination were found to decrease the migration of tumour cells by targeting two different pathways. This was shown to be significant with p values of 0.004, 0.0098 and 0.0021. Treated cells showed different fluorescence levels of actin and focal adhesions in comparison to untreated cells. In the presence of the drugs, actin was more highly condensed within the cytoplasm rather than on the surface of the cells, and the focal adhesions became more pronounced with less co-localisation of the two. This research has paved the way for future studies, in which anti-migratory drugs have the potential to be used at the surgical site, as a complement to conventional treatment, to ultimately prevent the onset of secondary tumours.

---

## Introduction

Glioblastoma Multiforme (GBM) is a form of malignant brain tumour (Figure 1), causing side effects ranging from personality changes to seizures, memory loss and mood disorders (Alexander & Cloughesy, 2017). Currently, only 5% of patients suffering from GBMs survive up to five years (Goodenberger & Jenkins, 2012) in comparison to melanoma and breast cancer at  $\sim 90\%$  (Siegel *et al.*, 2018), emphasizing the extent to which brain tumours are a national health issue. GBMs are relatively rare. The incidence of brain tumours over 2015-2017 was 12,071, in comparison to breast cancer, of which there were 55,176 new cases (CRUK, 2017). Therefore, less funding has been attributed to research in this area; Cancer Research UK (CRUK) spent as little as 2.7% of total funding on brain tumours in 2019/2020 (CRUK, 2020).

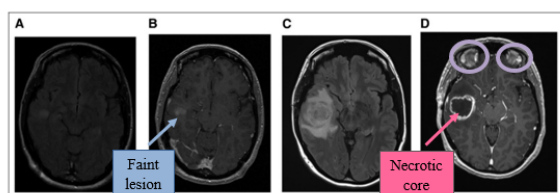


**Figure 1 | MRI images depicting progression of a brain tumour. (A,B)**

In the temporal lobe, the formation of a lesion is faintly visible at grades 1 and 2. (C,D) Ring-enhancing lesion with signs of

necrosis and peritumoral edemas, as shown by the purple circles, indicative of a GBM (Alexander & Cloughesy, 2017). This is graded as stage 4, in which the tumour is highly infiltrative and heterogenous (Goodenberger & Jenkins, 2012).

Current GBM therapies involve surgical resection of the tumour, radiotherapy, and chemotherapy with temozolomide. An issue often encountered with surgery is the incomplete resection of the tumour, in which the cells left at the surgical site migrate and disseminate into other regions of the brain. These cells go undetected in magnetic resonance imaging (MRI) scans after surgery, leading to the formation of secondary tumours (Forst *et al.*, 2014). Ninety percent of cancer deaths are attributable to metastasis or recurrence in the case of high-grade tumours (Sun *et al.*, 2015). This research provided a novel insight into the use of CCG-1423 and Rhosin hydrochloride as anti-migratory inhibitors for the purpose of overcoming long-term treatment failure and tumour recurrence. If placed at the surgical site via carmustine wafers, the motility of the remaining tumour cells could potentially be impeded until the patient can receive chemotherapy, typically two weeks after surgery has taken place.

## Drugs Targeting Migration

The motility of tumour cells relies heavily on the contraction of actin, induced by myosin II. In some instances, myosin is activated by the guanosine triphosphatase (GTPase), control protein 42 homolog (Cdc42), acting in combination with Rho and its effector, Rho-associated serine/threonine kinase (ROCK), to phosphorylate the myosin light chains (MLCs) (Kosla *et al.*, 2013). Actin contraction is regulated by the action of the GTPases, Rac and Rho. Rhosin

hydrochloride acts by suppressing the binding of RhoA to guanosine nucleotide exchange factors (GEFs) (Figure 2). Upon binding of the drug to the GEF sites, RhoA is maintained in an inactive state, in which guanosine diphosphate (GDP) remains bound. In a normal state, GEF binding activates RhoA upon catalysation of GDP to GTP. This in turn activates ROCK, enabling actomyosin contractility, regulation of the intermediate filaments through stress fibre formation, myosin II activation and re-positioning of the focal adhesions.

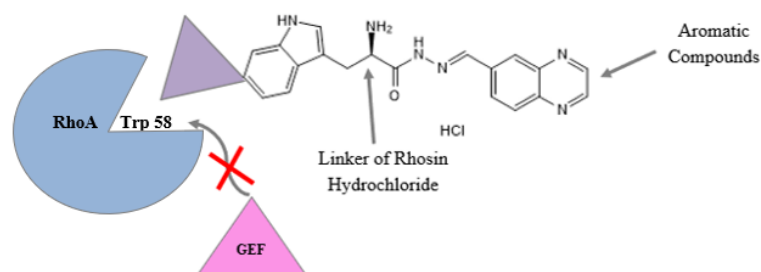


**Figure 2 | Chemical structure of Rhosin hydrochloride (Tocris, n.d.) and mechanism of action.** The aromatic compounds in Rhosin hydrochloride attach to the tryptophan 58 GEF binding sites on RhoA, inhibiting its activation. The compounds remain intact by a linker. The binding of Rhosin hydrochloride blocks GEF reaching the binding site of Rho GTPases (Shang *et al.*, 2012).

In cancer cells, RhoA is upregulated to enable migration. Rhosin hydrochloride acts to prevent this by inhibiting MLC phosphorylation, focal adhesion formation, and regulation of actin cytoskeleton dynamics. Unlike other anti-migratory drugs, Rhosin hydrochloride bypasses the

Cdc42 and Rac1 pathways (Biro *et al.*, 2014).

Cancer cells migrate by mesenchymal or amoeboid migration. Amoeboid migration bypasses the use of metalloproteinases to breakdown the extra cellular matrix. In mesenchymal migration, protrusions are

established by the polymerisation of actin to allow the cells to propel themselves forward (Gandalovičová *et al.*, 2017). Rac 1 induces the formation of new actin by activating the actin-related protein complex (Arp2/3) (Parri & Chiarugi, 2010). Rac1 and Cdc42 also activate Wiskott-Aldrich syndrome protein (WASP) and WASP-family verprolin-homologous proteins (WAVEs). WASP and WAVE act as the nucleating promoting factors by binding to actin and the Arp2/3 complex. Adhesion proteins, specifically integrins, are

relocated into the newly developed protrusions on the cancerous cells (Decaestecker *et al.*, 2006), alongside focal adhesions, to enable communication between the tumour cells and the ECM (Tojkander *et al.*, 2012). CCG-1423 targets a different cellular mechanism to RhoA hydrochloride, in which it inhibits serum response factor (SRF) by binding to oncogene megakaryoblastic leukaemia transcriptional co-activator protein 1 (MKL1), both of which are upregulated in cancer (Figure 3).

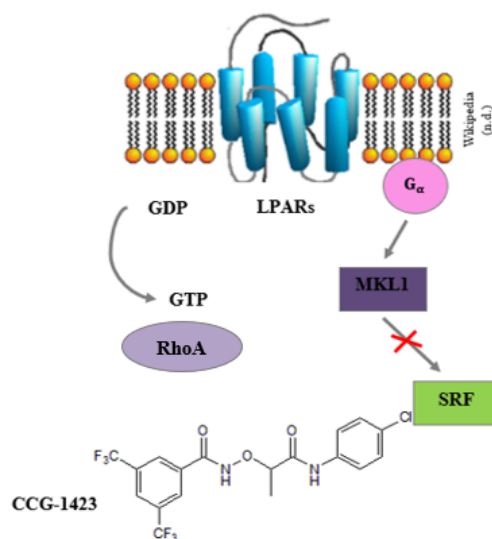


**Figure 3 | Chemical structure of CCG-1423 (Tocris, n.d.) and mechanism of action.**

Transcription of metastatic genes is induced by G-protein coupled receptor (GPCR) mediated RhoA activation, specifically by lysophosphatidic acid receptors (LPARs), and coupling to G-proteins, G $\alpha_{12}$ Q231L and G $\alpha_{13}$ Q226L (Vogt *et al.*, 2003). Activation of RhoA induces actin polymerisation and the dissociation of MKL1 into the nucleus. In an unbound state, MKL1 activates SRF to initiate gene transcription. CCG-1423 acts by inhibiting SRF (Evelyn *et al.*, 2007) and the localisation of MKL into the nucleus by binding to the nuclear localisation signal (NLS) region on MKL. This suppresses the binding of MKL1 to importin and MKL/SRF mediated gene transcription (Gau *et al.*, 2017).

MKL and SRF are also responsible for the synthesis of cytoskeletal regulatory proteins to enable remodelling of the actin for cell migration (Gau *et al.*, 2017). CCG-1423 prevents the interaction between MKL and SRF, suppressing the transcription of genes inducing migration and metastasis (Biro *et al.*, 2014). The drug also regulates MICAL2, a gene encoding F-actin monooxygenase, leading to the depolymerisation of actin (Gau *et al.*, 2017). Without these pathways, the cells cannot migrate as the polarity of the cell ceases to change and myosin II remains inactive (Evelyn *et al.*, 2007). The morphology of the migratory cancerous cells is also altered by CCG-1423, in which the protrusions are not as functional due to the depletion of ArpC2, vasodilator-stimulated phosphoprotein (VASP) and profilin 1, the actin-binding proteins involved in the formation of the cellular extensions (Gau *et al.*, 2017).

### **Other Publications on CCG-1423 and Rhosin Hydrochloride**

Previous studies showed the effects of drugs acting individually against various forms of cancer. Rhosin hydrochloride was previously studied on MCF7 breast cancer cell lines by Shang *et al.*, where it was found to reduce the expression of RhoC and RhoA to suppress migration (Shang *et al.*, 2012). Evelyn *et al.* reported that CCG-1423 inhibited invasion and migration in the PC-3 prostate cancer cell line by suppression of SRF and MKL1 gene transcription (Evelyn *et al.*, 2007). This was

the first scientific publication to introduce CCG-1423 as a potential anti-migratory drug. Although successful in other cancer cell lines, CCG-1423 proved ineffective in glioma cells and failed to inhibit migration as described by Ketchen *et al.* This paper proposed that a mesenchymal to amoeboid transition (MAT) occurred, in which the cancerous cells adapted their mode of migration to evade the effects of CCG-1423 (Ketchen *et al.*, 2020). This highlighted the importance of using the drugs in combination to target both mechanisms. Rhosin hydrochloride would act to target amoeboid migration and CCG-1423 mesenchymal migration.

## **Methodology**

### **Cell Culture**

The established glioma cell line U87 (ATCC, STR profiled and mycoplasma negative) was grown at 37°C in a 5% carbon dioxide (CO<sub>2</sub>) incubator. The cells were cultured in 10ml Dulbecco's Modified Eagle medium (DMEM, Sigma) with a medium-high glucose content, 10% (v/v) foetal calf serum (FCS, Sigma) and 1/100 penicillin and streptomycin (Sigma).

The cancerous cells had a starting cell density of  $2 \times 10^6$ . U87 monolayers nearing confluency were passaged weekly at 1/20, in Nuair class II biosafety cabinets. The supernatant was removed

from cultured U87 cells and the cells were washed with 5ml phosphate buffered saline (PBS, Sigma). Cells were incubated at 37°C for 5 minutes with 1ml Trypsin (Sigma) prior to dilution with 9ml DMEM. In a T75 flask, 1ml of the passaged cells were added to 9ml of fresh DMEM solution.

### Scratch Wound Assays

The assay was performed following the protocol cited in a paper by Liang *et al.*, 2007. Scratch wound assays were performed by seeding  $1 \times 10^5$  cells/ml in 6 well plates (Corning). The average number of cells in the culture was measured using a haemocytometer at x10 magnification to determine the volume of cells required. The remaining volume was made up with DMEM. Each well contained 2ml cell suspension. Cells were incubated at 37°C for 24 hours. The scratch was applied with gentle pressure using a p200 pipette tip (Starlab). 2µl of dimethyl sulfoxide (DMSO, Sigma) were added to the control. Cells were exposed to 2µl of CCG-1423 (500nm, Tocris) and 2µl of Rhosin hydrochloride (1µM, Tocris) for individual and combination treatment. Imaging of the scratch area was gathered using the EVOS imaging system (ThermoFisher) at x4 magnification over 24h. The protocol was modified, such that the cells were not

washed with PBS to prevent disturbance to the glioma cells.

### Tumour Spheroid Assays

Tumour spheroids were composed of monolayer cancerous cells to form a 3D structure, resembling a tumour. The spheroids were embedded in a collagen matrix to mimic the environment of the brain. This provided an *in vitro* 3D model of a tumour within the brain. To generate 3D spheroids, the protocol according to Cockle *et al.*, 2015 was used. Cells were diluted to  $5 \times 10^3$  cells/ml in DMEM, and 200µl of the cell suspension was added to each well in a 96 well low adherence plate (Nunc). Incubation of the cells was carried out for 5 days at 37°C. For the assay, preparation of the collagen matrix consisted of chilled 10.4ml collagen (Rat tail, type I, Corning), 1.52ml 5x DMEM and 72µl of 1M sodium hydroxide (NaOH, Sigma). The suspension was mixed by gentle pipetting with a Gilson pipette. 190µl of cell suspension was removed from the wells with a multichannel pipette (Eppendorf) prior to being replaced by 100µl of collagen matrix suspension and incubated for 10 min. 6µl of DMSO was added to the control wells, along with 6µl of CCG-1423 (500nM) and 6µl of Rhosin hydrochloride (1µM) for both the individual and combination treatment. Imaging of the

spheroids was taken over 72h using an EVOS imaging system microscope at a magnification of x10.

### **Paraformaldehyde Fixation and Immunofluorescence (IF)**

Fixation and IF was carried out according to “Immunofluorescence/Live cell imaging” by Anke Brüning-Richardson. In preparation for confocal imaging, monolayer cells were fixed. Wells in 6 well dishes (Nunc) were seeded with 2ml cell suspension and a scratch was applied over the centre of the cover slip. The scratch assay was carried out as described before. Fixation of the cells on the cover slips required the addition of 4% paraformaldehyde (PFA, Sigma) and incubation for 20 min at room temperature (RT). Cells were incubated with 0.1% PBS-Triton X-100 for 5 min after fixing. Cells were then washed three times with PBS. IF was achieved by adding blocking solution (Marvel milk powder) to the wells, a combination of PBS and 0.1% milk powder. Phalloidin 594 dye (Merck Millipore) for binding to actin, mouse anti-vinculin antibody (Merck Millipore) for focal adhesion staining and 4', 6-diamidino-2-phenylindole stain (DAPI, Merck Millipore) for binding to deoxyribonucleic acid (DNA) were used in the first incubation step. The secondary antibody

used was Alexa Flour anti-mouse 488 (Invitrogen). Antibodies were prepared by addition to the blocking solution and centrifugation for 5 min. For each antibody, 200µl of the supernatant was added to parafilm in make-shift incubation chambers and covered with the cover slip from the wells, applied face down. Antibodies were incubated one at a time in the dark for 1h time periods. Cover slips were washed with PBS in between each use. Following the first incubation step, the cells were washed 3x in PBS and again incubated as before in the secondary antibody solution, consisting of 200µl of the secondary antibody. After 3 washes with PBS, the cover slips were mounted on glass slides with Fluoromount G (Thermofisher) for imaging.

### **Fixation of Spheroids**

Preparation of spheroids for confocal analysis followed the protocol according to Harmer *et al.*, 2019. The medium was removed from spheroid assays. After washing 3x with PBS, fixation was carried out in the same way with 4% PFA but for an incubation of 24h in the dark at RT in the original 96 well plate. Next, spheroids in their collagen plugs were incubated with 100µl of 0.1 % Triton X-100 in PBS for 30 min at RT. Washing of the cells with 3x PBS in between the addition of reagents was carried out. The blocking solution that

was used contained 0.05% skimmed milk powder and 1x PBS. Incubation of cells with 100µl blocking powder occurred for 15 min. The primary antibody mouse anti-vinculin (Merck Millipore) and actin and DNA dyes (Merck Millipore) were prepared in the same way as the scratch assay fixation with the same incubation periods, but in this case 50µl of antibody and dye solution were added to each well as a mixture twice. The second incubation period with Alexa Fluor anti-mouse 488 (Invitrogen) was 1h 30 min. Spheroids in their original collagen were washed with PBS before being mounted onto cover slips.

### **Confocal Imaging**

Cells and spheroids were imaged using Nikon A1R confocal imaging. This was carried out by Philippa Vaughn-Beaucaire, a PhD researcher at the University of Huddersfield.

### **ImageJ**

Migration of the cells in the scratch wound assay was determined by ImageJ (<https://imagej.nih.gov/ij/>). The area of the scratch was measured and the percentage change of each relative to the control was calculated.

Migration of the cancerous cells from the spheroid was determined by measuring the area of the spheroid core, the invasion front

and the invasion edge. The migration index of the invasion front and edge was calculated in comparison to the spheroids at 0h (Cockle *et al.*, 2015).

For the confocal image analysis, the fluorescence of actin and focal adhesions in each cell was quantified with ImageJ. The corrected total fluorescence count (CTFC) for each condition was calculated and compared to the control. Actin fluorescence was measured by counting the number of cells with actin on the cell surface, in which the actin was more cortical, and the number of cells with actin relocated to the cytoplasm. This determined the movement of actin during cell migration.

### **Statistical Analysis**

Results were analysed using Microsoft Excel 2016. A two-sample t-test assuming unequal variance was used to determine if there was a difference between the control and treatment for the scratch wound assay, tumour spheroid assay and confocal analysis. A p value of <0.05 was denoted as significant. For non-parametric data in the analysis of the confocal imaging, chi-squared tests were conducted with a p value of <0.05.

## Results

### Migration in a 2D Model

The migration of treated U87 tumour cells and untreated cells with the addition of DMSO only were analysed using scratch wound assays over intervals of 0h, 6h and 24h to establish if combination treatment was more effective than the drugs acting individually. The migration was calculated comparative to the area of the wound at 0h

for each variable. The assays were replicated in triplicate over three separate days and an average was taken. The migration of the tumour cells treated in combination was significantly reduced in comparison to the control after 24h ( $p = 0.004$ ) (Figure 4). The drugs had minimal effect on suppressing the migration of the cancerous cells when used individually.

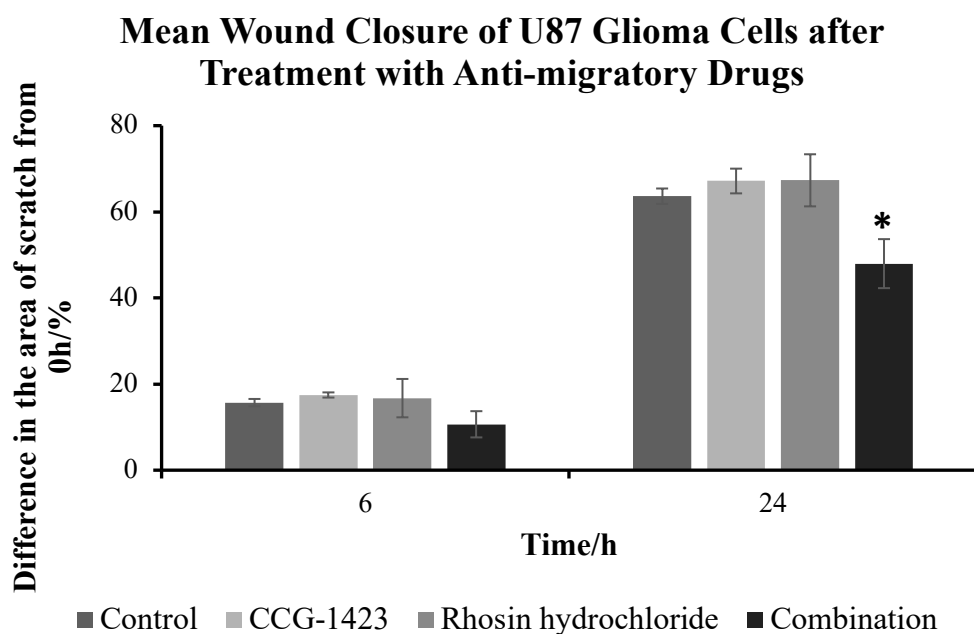


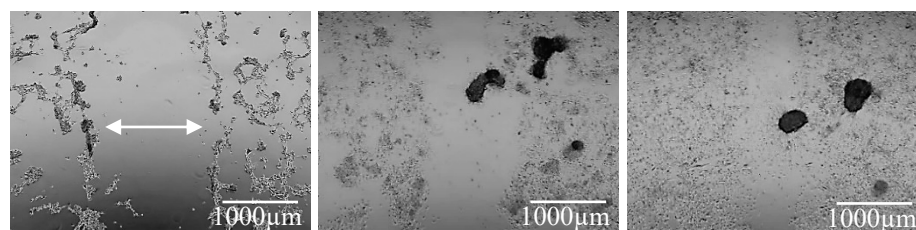
**Figure 4 | Percentage scratch wound closure of treated and untreated glioma cells.** The migration of the cells into the scratch wound was significantly smaller when the drugs were used in combination ( $p = 0.0042$ ) in comparison to the control. When treated with CCG-1423 and Rhosin hydrochloride individually, the wound closed by 67% of its original area after 24h. This was as minimal as 48% when used in combination. (\*) indicates that the result was significantly different from the control with a  $p$  value of  $< 0.05$ .

---

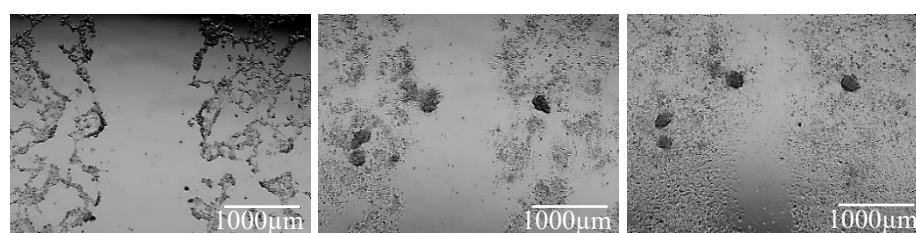
The scratch wounds were visualised using EVOS imaging at x4 magnification

(Figure 5) to quantify the extent of migration for treated and untreated cells.

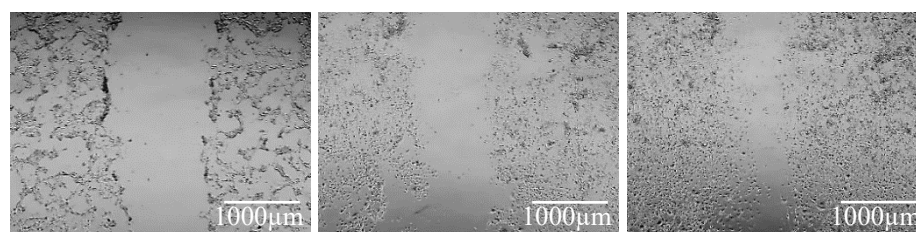
---



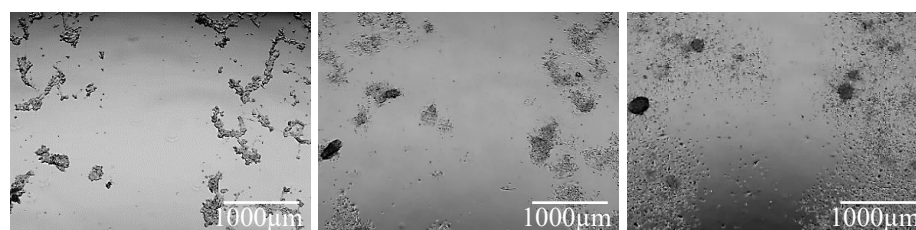
(A) (B) (C)  
Untreated U87 glioma cells (A) 0h (B) 6h (C) 24h



(D) (E) (F)  
CCG-1423 treated U87 glioma cells (D) 0h (E) 6h (F) 24h



(G) (H) (I)  
Rhosin hydrochloride treated U87 glioma cells (G) 0h (H) 6h (I) 24h



(J) (K) (L)  
Combination treated U87 glioma cells (J) 0h (K) 6h (L) 24h

**Figure 5 | Imaging of scratch wound assays at x4 magnification.** Glioma cells treated with the drugs in combination exhibited the least wound closure after 24hr (L) comparative to the control (C) and the individual treatment (F & I). The area of the scratch used is highlighted (A).

---

### Migration in a 3D Model

Tumour spheroid assays were performed to compare the effect of the drugs on cell migration in a 3D environment to the 2D scratch assays. The spheroid assay gave a better representation of the tumour cells in a 3D structure within the brain as mimicked by the collagen matrix. The area of the core, invasion front and invasion edge of the spheroids (Figure 6) were measured using ImageJ at 0h, 24h, 48h and 72h. From these values, the average migration index of both the invasion front (Figure 8) and the invasion edge (Figure 9) was calculated using the equation:

$$\text{Migration index} = \frac{\text{Area of the core}}{\text{Area of the core} + \text{Area of the invasion front} + \text{Area of the invasion edge}}$$

The migration index gives a value between 0 and 1, in which a value of 1 denotes the highest level of migration.

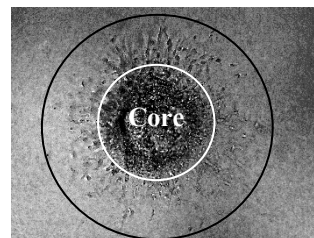


**Figure 6 | Core, invasion front and invasion edge of a tumour spheroid.** The inner white circle represents the invasion front, consisting of 75% of the migratory cells. The black outer circle shows the invasion edge, consisting of the remaining 25% of migratory cells.

Spheroids treated with Rhosin hydrochloride and CCG-1423 in combination had the smallest fold change in the size of the core over 72h in comparison to the control and individual treatment (Figure 7). The increase in core size is caused by the proliferation of the cancerous cells. As the core size increases, the tumour cells in the bulk of the core become hypoxic, leading to necrosis of the cells. As the difference between the change in the core of untreated cells compared to treated cells was insignificant, this showed that the drugs purely targeted cell migration and not proliferation.

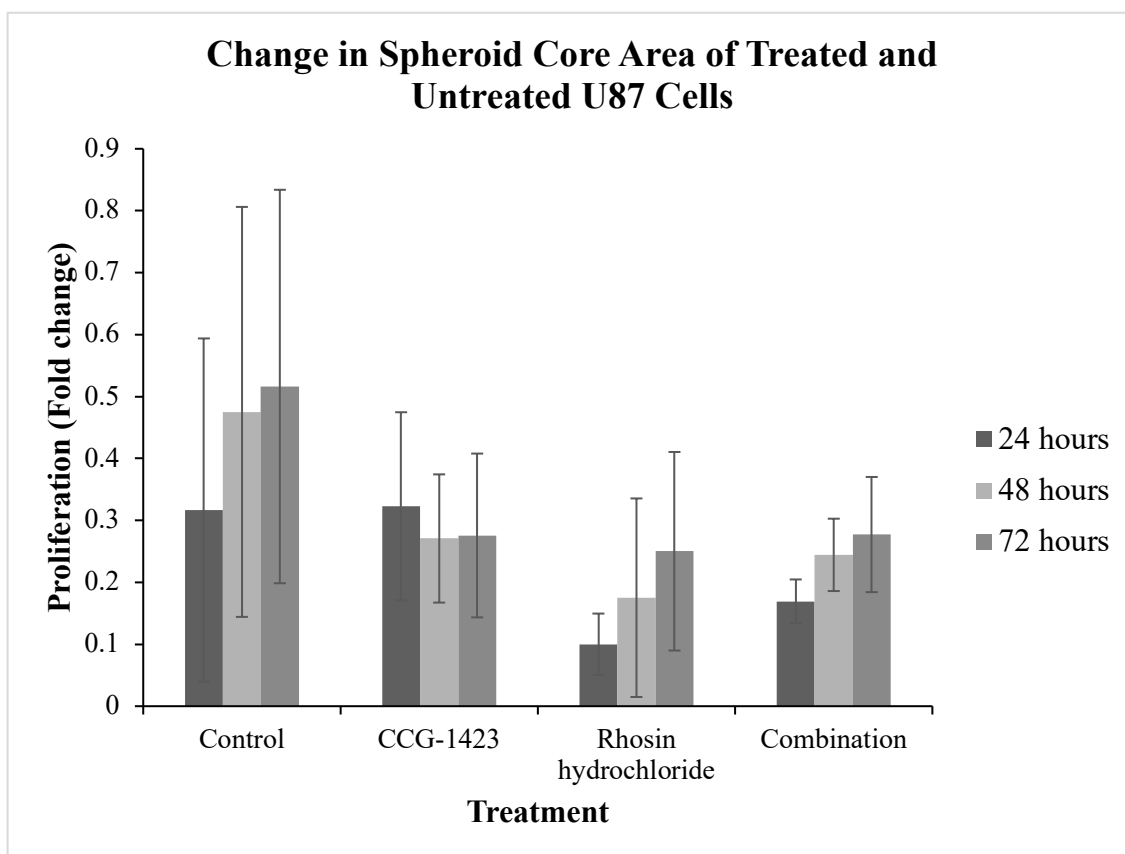


**Figure 7 | Proliferation of the spheroid core of treated and untreated U87 glioma cells over 72h.** The core of the spheroid of glioma cells treated with DMSO had a fold change of approximately 0.52 after the 72h period. For combination treatment, cell proliferation was reduced, evidently as the fold change was only 0.28 after 72h ( $p = 0.053$ ). However, this result was not significant.

The migration index of the invasion front (Figure 8) and edge (Figure 9) was calculated to represent the migration of tumour cells within the brain as a whole invasive front and as single, fast migrating cells. It was found that combination treatment successfully inhibited both cell

migration types, which confirmed drug activity in a 2D environment. On the other hand, when using the drugs individually, migration was not affected. This confirmed the theory that the drugs should be further tested in combination for potential brain tumour therapies.

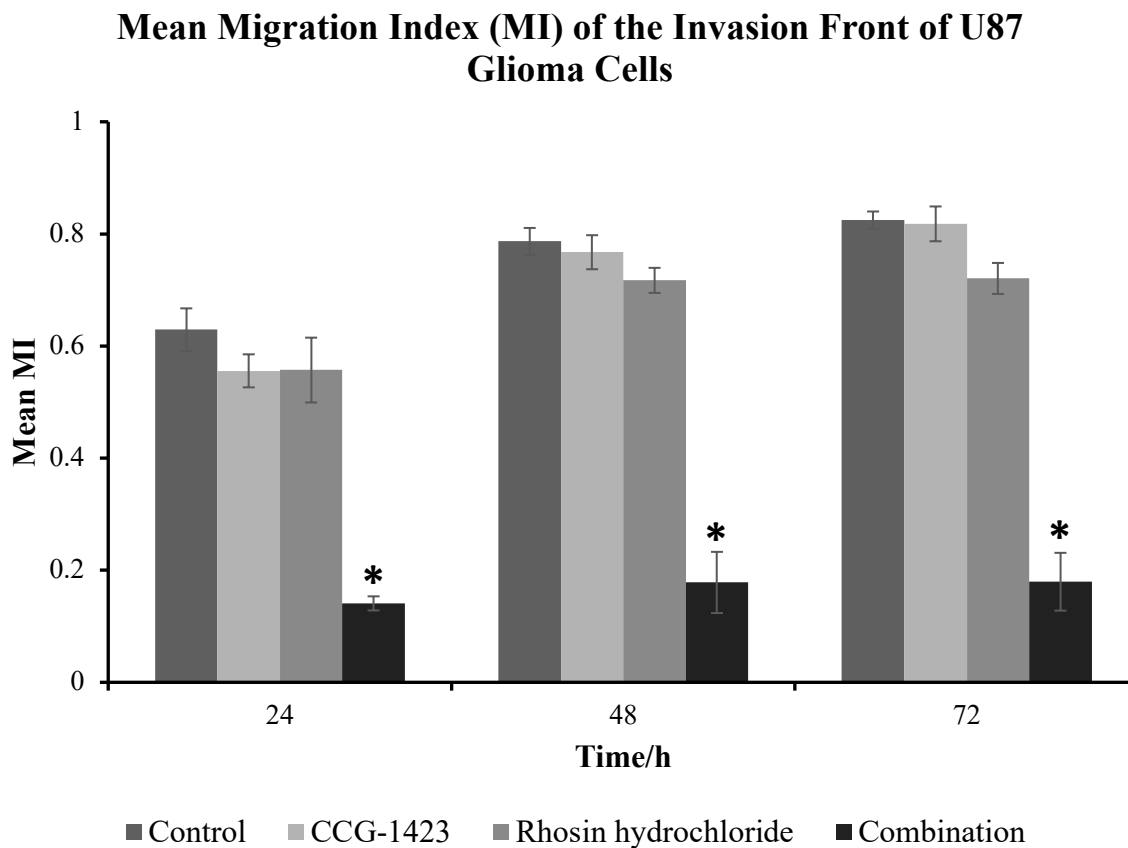


**Figure 8 | Migration index of the invasion front of the spheroids of treated vs untreated tumour cells.** CCG-1423 and Rhosin hydrochloride used in combination significantly reduced the migration of the cells away from the spheroid ( $p = 0.0098$ ). In combination, the mean migration index was 0.18, compared to the control which was 0.82.

---

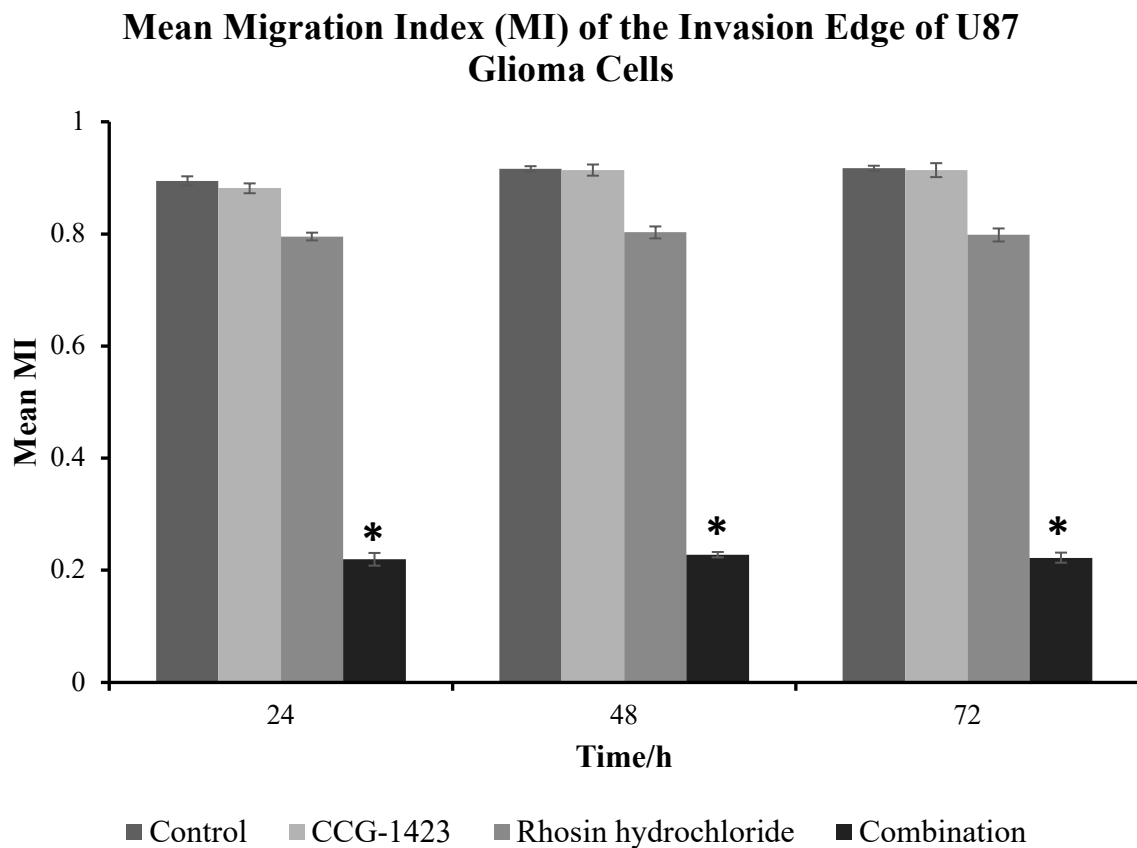


**Figure 9 | Migration index of the invasion edge of the spheroids.** CCG-1423 and Rhosin hydrochloride had little effect on inhibiting the migration of the cells when used individually. In combination, the migration index was significantly lower than that of the control ( $p = 0.00205$ ).

The spheroids were imaged using the EVOS imaging system (Figure 10). Eight repeats were taken for each variable. When using the drugs in combination, six of these repeats had a migration index of zero, showing the effectiveness of this treatment.

Although there were no migratory cells from the combination treatment, the size of the core increased, potentially due to the inability of tumour cells to detach from the main bulk of the tumour. Spheroid images of the control and individual treatment showed extensive migration away from the core.

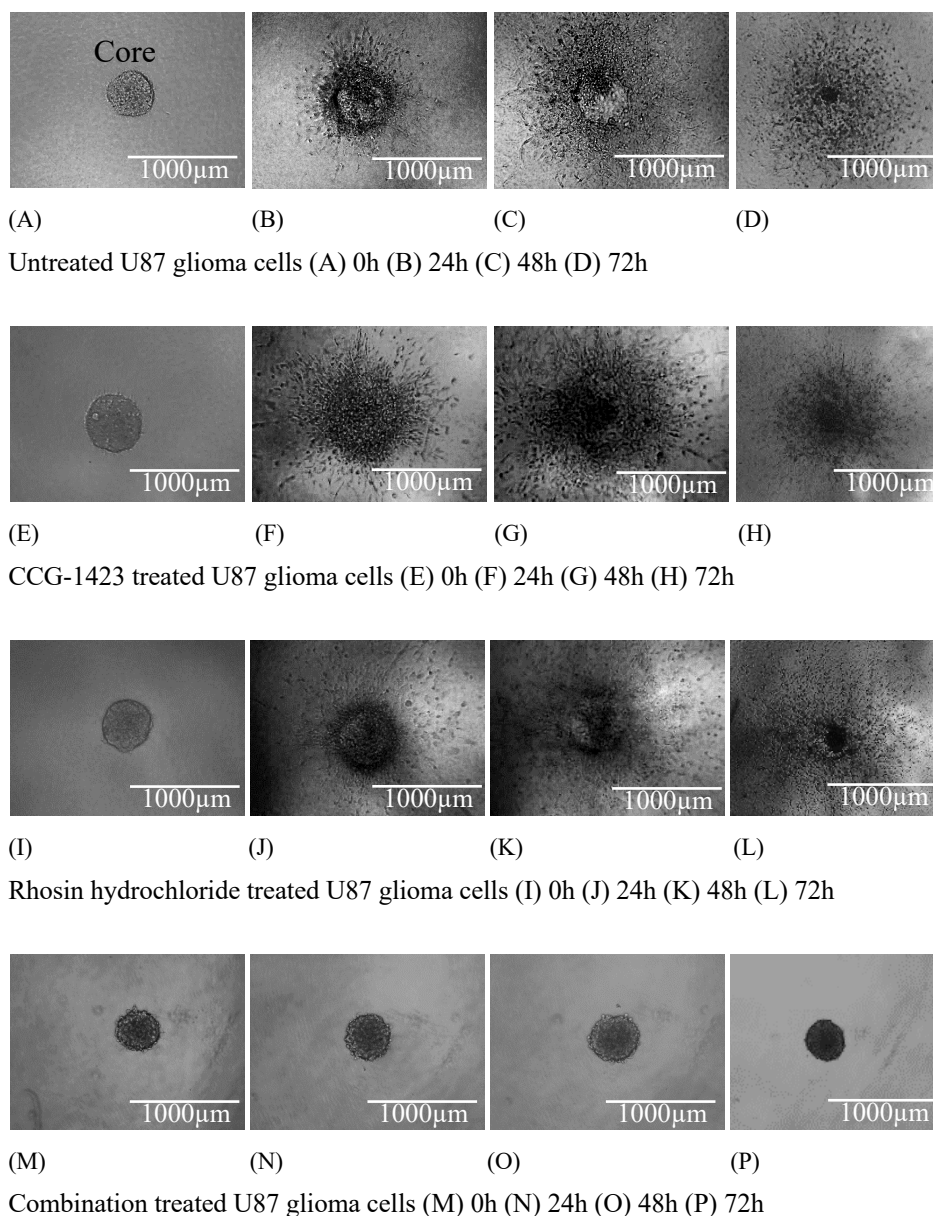


**Figure 10: Imaging of the spheroids at x10 magnification.** Spheroids were imaged for analysis with ImageJ. Rhosin hydrochloride and CCG-1423 inhibited migration when added to glioma cells in combination.

---

### Confocal Analysis

Confocal analysis was used to investigate the effect of CCG-1423 and Rhosin hydrochloride at the cellular level. Cells were labelled with phalloidin 594 for visualisation of actin localisation and

mouse anti-vinculin antibody for focal adhesion localisation. The average immunofluorescence intensity of the migratory cells was calculated for the control and treated glioma cells to determine the expression levels of the proteins. This was performed both for the

---

migratory cells at the outer edge of the scratch wounds (Figure 11) and those present in the tumour spheroids (Figure 12). The cells from the scratch wound assay had a lower CTCF when treated with CCG-1423 and Rhosin hydrochloride than the

control. Conversely, for the tumour cells within the spheroids, actin and focal adhesions were more highly expressed when the drugs were used in combination than in the untreated cells.

---

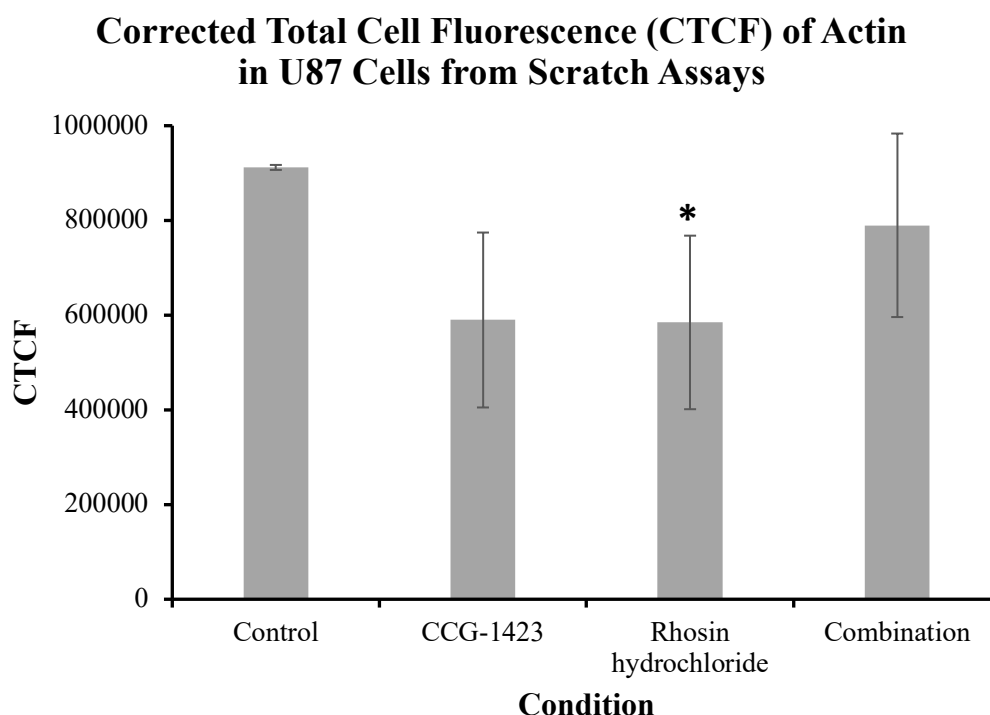


**Figure 11 | Average cell fluorescence of the migratory cells in the scratch wound.** Cells were labelled with phalloidin 594 to detect actin and mouse anti-vinculin antibody for focal adhesions. The control exhibited the highest CTCF at approx. 912,000. Tumour cells treated with Rhosin hydrochloride had significantly reduced protein expression of actin ( $p = 0.012$ ) in comparison to the control.

---

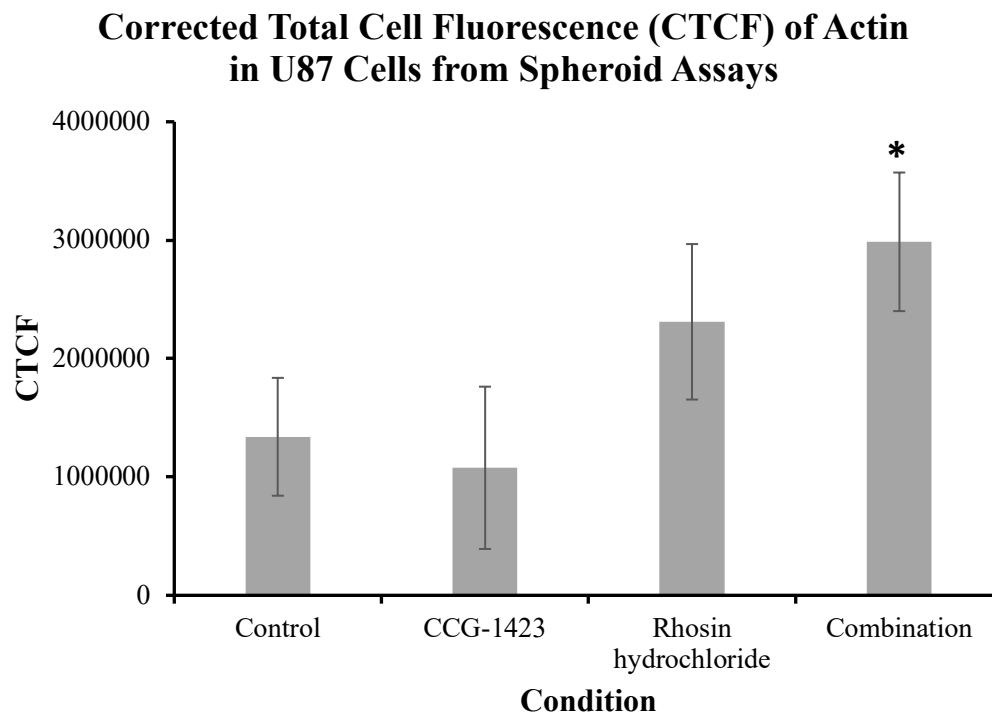


**Figure 12 | Average cell fluorescence of the migratory cells in the spheroids in treated and untreated tumour cells.** Actin was labelled with phalloidin 594 and the focal adhesions with a mouse anti-vinculin antibody. There was no significant difference between the control and the drugs used individually. In combination, the highest expression levels of actin were visible ( $p = 0.012$ ).

After quantitative analysis, the pattern of actin within the cell, its distribution and interaction with focal adhesions was observed. Qualitative analysis was used to visualise if drug activity targeted migration by exerting an effect on the localisation and distribution of actin, focal adhesions, or both. In 2D models, there was no difference in the distribution of actin for the treated

cells, in comparison to the control, in which it was compacted on the cell surface. However, in the 3D spheroids, Rhosin hydrochloride and the drugs used in combination caused the actin to relocate to the cytoplasm. For the control and CCG-1423 treated cells, the actin was more cortical (Figure 13). This is suggestive of the possibility that Rhosin hydrochloride inhibits migration by targeting actin.

### Percentage of Cells in the Spheroid Assay with Actin on the Cell Surface

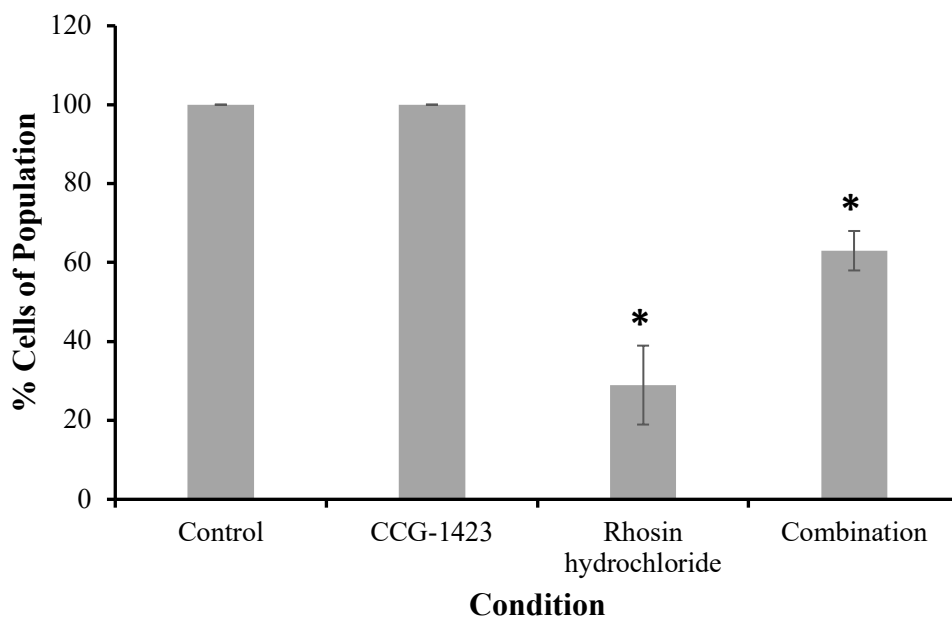


**Figure 13 | Confocal imaging analysis of the distribution of actin in the migratory cells of spheroids.** CCG-1423 had no effect on the distribution of actin. Rhosin hydrochloride and the drugs used in combination had a significantly different distribution of actin from the control, in which it was relocated to the cytoplasm rather than on the cell surface.

In the control for both the migratory cells at the wound site and in the spheroids, the actin was distributed on the cell surface and co-localised with the focal adhesions to produce a yellow hue on the outer edge of the cells (Figure 14A, Figure 15A). The actin had no visible stress fibres and the cell bodies were elongated and oval.

#### Scratch Wound Confocal Analysis

The cells for both treated and untreated glioma cells appeared uniform. However, when treated with Rhosin hydrochloride,

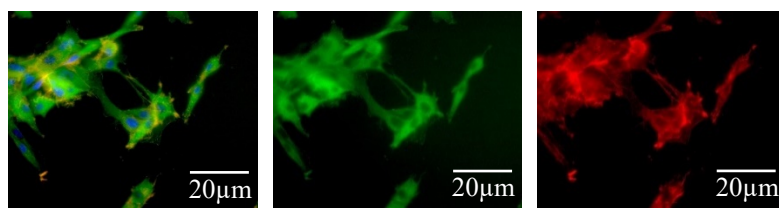
stress fibres were present (Figure 14G). In combination, the cancerous cells formed clusters (Figure 14H) with longer extensions, which are potentially filopodia. Although protrusions aid migration, the binding of Rhosin hydrochloride to the GEF binding pocket suppresses actomyosin contractility, hence migration cannot occur.

#### Spheroid Confocal Analysis

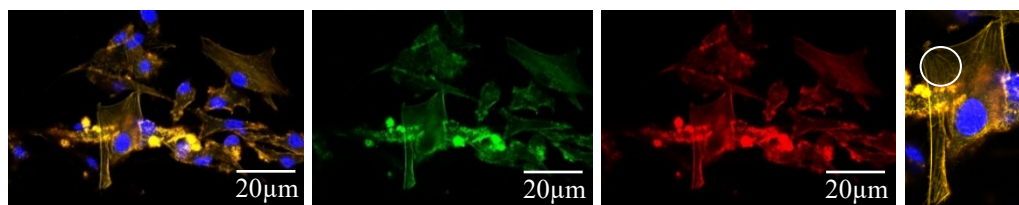
Cells treated with CCG-1423 exhibited similar properties to the control except for some cells consisting of extensions of focal

adhesions and actin (Figure 15E and Figure 15H). The focal adhesion stain in the control was more diffused on the surface of the migratory cells. In comparison, the focal adhesion in the treated cells appeared more pronounced, indicating that Rhosin hydrochloride affected focal adhesion

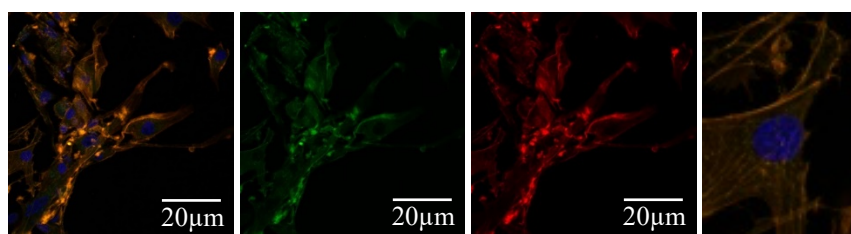
dynamics. In Rhosin hydrochloride treated tumour cells, the cells were elongated and appeared bigger than the untreated cells with visible clusters (Figure 15Q). In some cells, there were visible stress fibres of actin (Figure 15K). This was the case for spheroids treated in combination.



(A) (B) (C)  
Untreated U87 glioma cells (A) Merged (B) Focal Adhesions (C) Actin

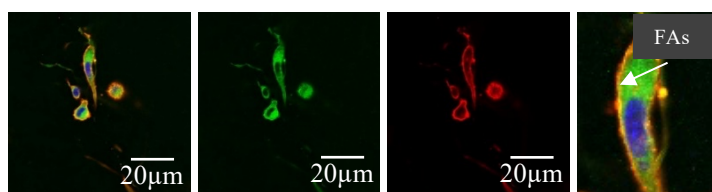


(D) (E) (F) (G)  
Rhosin hydrochloride treated U87 glioma cells (D) Merged (E) Focal Adhesions (F) Actin (G) Stress Fibres

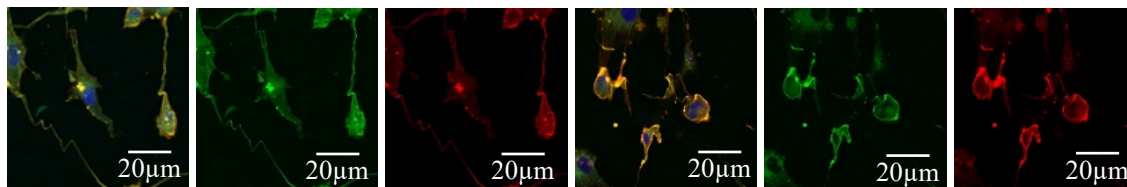


(H) (I) (J) (K)  
Combination treated U87 glioma cells (H) Merged (I) Focal Adhesions (J) Actin (K) Stress Fibres

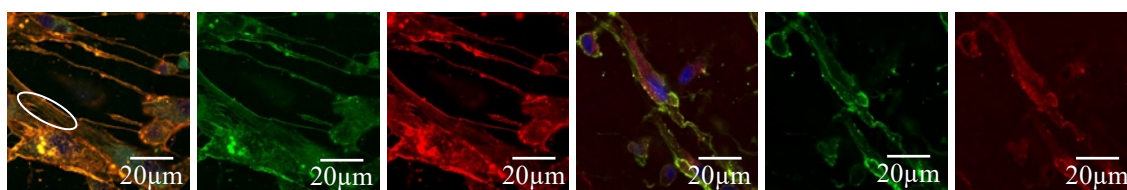
**Figure 14 | Confocal imaging of migratory cells at the scratch wound site.** The control images were provided by Anke Brüning-Richardson, the research group leader, at the University of Huddersfield. CCG-1423 was excluded from the results as the antibodies did not bind to the cells effectively enough to generate a fluorescence. (G) Circle highlights the stress fibres.



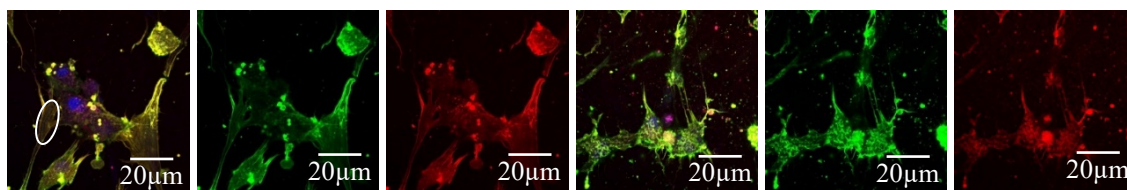
(A) (B) (C) (D)  
 Untreated U87 glioma cells (A) Merged (B) Focal Adhesions (C) Actin (D) Focal Adhesions



(E) (F) (G) (H) (I) (J)  
 CCG-1423 U87 glioma cells (E & H) Merged (F & I) Focal Adhesions (G & J) Actin



(K) (L) (M) (N) (O) (P)  
 Rhosin hydrochloride treated U87 glioma cells (K & N) Merged (L & O) Focal Adhesions (M & P) Actin



(Q) (R) (S) (T) (U) (V)  
 Combination treated U87 glioma cells (Q & T) Merged (R & U) Focal Adhesions (T & V) Actin

**Figure 15 | Confocal imaging of the migratory cells in the spheroids.** Rhosin hydrochloride and the drugs in combination affected the structure of actin, which was apparent by the formation of stress fibres as circled (K, Q). The control images from an experiment run in parallel were provided by Glory Duru, a former student at the University of Huddersfield.

## Discussion

Cancer treatments are often less successful than predicted from pre-clinical studies due

to the ability of cancer cells to adapt to adverse environments and challenges, such as the exposure to chemotherapeutic drugs.

This study provided novel research into how to improve the efficacy of existing drugs. The experimental analysis of CCG-1423 and Rhosin hydrochloride proved that in combination the drugs significantly reduced the migration of cells compared to individual use by targeting two different signalling pathways for cell migration. This was exhibited in both 2D scratch assays and 3D tumour spheroid assays. The scratch wound closed by 48% when using the drugs in combination compared to a wound closure of 67% for the control ( $p = 0.004$ ). For the spheroid assays, cancerous cells treated with the drugs in combination had a migration index (MI) of 0.18 for the invasion front and 0.22 for the invasion edge. The MI of the invasion front for control cells was 0.82 and 0.92 for the invasion edge ( $p = 0.0098$  and  $0.0021$ ). Both models showed that the motility of cancerous cells was successfully inhibited by combination treatment, but not when the drugs were used individually.

Interestingly, the Rhosin hydrochloride treated and combination treated cells displayed stress fibres across the whole cell bodies, which are necessary to produce the contractile forces to pull the cell forwards. The generation of stress fibres is caused by the phosphorylation of MLCs (Vallénus, 2013). This was expected for Rhosin as the assays showed that the migration of the

cells was not inhibited. However, this was unusual for the combination treatment. The formation of stress fibres is essential for migration in mesenchymal migration. The pattern emerged potentially because of the actin dispersing within the focal adhesions. As these were present in Rhosin hydrochloride treated cells and not CCG-1423 treated cells, this may be indicative that CCG-1423 activity targets the mesenchymal pathway but not amoeboid migration. This would explain why CCG-1423 did not inhibit migration on its own.

Confocal imaging analysis showed that the drugs altered the expression levels of actin in the cancerous cells. The corrected total cell fluorescence (CTCF) of migratory cells at the site of the scratch wounds was 912,000 for the control, compared to a lower CTCF of 790,000 for cells treated with Rhosin hydrochloride ( $p = 0.012$ ), showing that the drug reduced the expression of actin. The migratory cells taken from the spheroids treated with the drugs in combination had an average CTCF of 3,000,000 with a higher expression level of actin, compared to the control with a CTCF of 1,340,000 ( $p = 0.012$ ).

Analysis of the migratory cells in the spheroids revealed that in the presence of the drugs, the cells had more pronounced focal adhesions on the surface. The

diffusion of the focal adhesions in the migratory cells in the control may be due to a biological phenomenon known as ‘focal adhesion dynamics’. In this process, at the leading edge of the cell, the focal adhesions are well established to allow the cell to interact with the ECM and transfer signals across itself. The assembly of the focal adhesions at the front of the cell recruits other proteins, specifically vinculin which informs the cell of the rigidity of the ECM, so that the cell can progress with migration. However, towards the rear of the cell, the focal adhesions are disassembled to allow the cell to migrate forwards. The size of focal adhesions changes because of the turnover of associated proteins, which is the rate at which new proteins are synthesised after the degradation of old ones. The focal adhesions bound to the ECM are large, whereas disassembled focal adhesions are small to allow motility (Maziveyi & Alahari, 2017). In the treated cells, the focal adhesions were well established, hence the cell potentially could not migrate as there was no disassembly of the focal adhesions.

For the scratch assay, in the Rhosin hydrochloride and combination treated cells, there was less co-localisation of actin and focal adhesions. Actin dynamics are very similar to focal adhesion dynamics, in which actin is recruited to the leading edge and polymerised. During the migration of a

cell, actin and focal adhesions follow one another in that they are highly distributed at the leading edge and less so within the cell (Tojkander et al., 2012). This explains why in the control cells, the focal adhesions and actin were co-localised. The drugs in combination on the spheroid and scratch wound assays changed the cytoskeleton and cellular dynamics. This is indicative of the possibility that the cells may have induced a switch to a different mode of migration, known as collective cell migration.

In this study, 2D and 3D models provided different insights into the action of migration. Collagen in spheroid assays was representative of the ECM in the brain. With combination treatment, the cancerous cells were not motile, indicating that actin and RhoA were inhibited to prevent the production and secretion of MMPs as well as their adoption to an amoeboid, ‘path finding’ migratory phenotype. Further studies with enzyme immunoassays and mass spectrometry could test this theory by detecting the levels of MMP. Focal adhesion turnover inhibition could only be assessed in scratch wound assays as the collagen is semi-solid. An example of this is that fewer integrins are needed to be in contact with the surface and allow migration, as there are fewer contractile forces (Harunaga & Yamada, 2011).

## Conclusion

The mechanisms by which Rhosin hydrochloride and CCG-1423 work were already known in terms of their effect on intracellular events and molecules. However, this study outlined their effects on cytoskeletal proteins as well, specifically focal adhesions and actin. This is a scientific breakthrough for brain tumour research as the current treatments are unsuccessful in prolonging the lives of patients with GBM for longer than 1.5 years, which is highly devastating. The drugs investigated here have the potential to stop migration at the site of surgical removal of the tumour to prevent tumour recurrence and formation of secondary tumours.

## Acknowledgements

Thank you to Anke Brüning-Richardson for the support throughout the project both within the laboratory and externally. It was an honour to be part of such exciting research into a very prevalent disease. I would also like to thank Philippa Vaughn-Beaucaire for guidance on the protocols and for dedicating more time when I required additional hours in the laboratory.

## References

- Alexander, B.M., Cloughesy, T.F. (2017). Adult glioblastoma. *Journal of Clinical Oncology*, 35(21), 2402-2409. doi:10.1200/JCO.2017.73.0119
- Brüning-Richardson, A. *Immunofluorescence/Live cell imaging*. personal communication. (April 2020). University of Huddersfield.
- Biro, M., Munoz, M., Weninger, W. (2014). Targeting Rho-GTPases in immune cell migration and inflammation. *British Journal of Pharmacology*, 171(24), 5491-5506. doi:10.1111/bph.12658
- Cancer Research UK (2017) Statistics by cancer type. Retrieved from <https://www.cancerresearchuk.org>
- Cancer Research UK (2020) How much we spend on research. Retrieved from <https://www.cancerresearchuk.org>
- Decaestecker, C., Debeir, O., Van-Ham, P., Kiss, R. (2006). Can anti-migratory drugs be screened *in vitro*? A review of 2D and 3D assays for the quantitative analysis of cell migration. *Medicinal Research Reviews*, 27(2), 149-176. doi:10.1002/med.20078
- Evelyn, C., Wade, S., Wang, Q., Wu, M., Iniguez-Lluhi, J., Merajver, S., Neubig, R. (2007). CCG-1423: a small-molecule inhibitor of RhoA transcriptional signaling. *Molecular Cancer Therapeutics*, 6(8), 2249-2260. doi:10.1158/1535-7163
- Evelyn, C.R., Bell, J.L., Ryu, J.G., Wade, S.M., Kocab, A., Harzdorf, N.L., Hollis Showalter, H.D.H., Neubig, R.R., Larsen,

- S.D. (2010). Design, synthesis and prostate cancer cell-based studies of analogs of the Rho/MKL1 transcriptional pathway inhibitor, CCG-1423. *Bioorganic & Medicinal Chemistry Letters*, 20(2), 665-672. doi:10.1016/j.bmcl.2009.11.056
- Forst, D.A., Nahed, B.V., Loeffler, J.S., Batchelor, T.T. (2014). Low-grade gliomas. *The Oncologist*, 19(4), 403-413. doi:10.1634/theoncologist.2013-0345
- Gandalovičová, A., Rosel, D., Fernandes, M., Veselý, P., Heneberg, P., Čermák, V., Petruželka, L., Kumar, S., Sanz-Moreno, V., Brábek, J. (2017). Migrastatics- anti-metastatic and anti-invasion drugs: promises and challenges. *Trends in Cancer*, 3(6), 391-406. doi:10.1016/j.trecan.2017.04.008
- Gau, D., Veon, W., Capasso, T., Bottcher, R., Shroff, S., Roman, B., Roy, P. (2017). Pharmacological intervention of MKL/SRF signaling by CCG-1423 impedes endothelial cell migration and angiogenesis. *Angiogenesis*, 20(4), 663-672. doi:10.1007/s10456-017-9560-y
- Goodenberger, M., Jenkins, R. (2012). Genetics of adult glioma. *Cancer Genetics*, 205(12), 613-621. doi:10.1016/j.cancergen.2012.10.009
- Harunaga, J., Yamada, K. (2011). Cell-matrix adhesions in 3D. *Matrix Biology*, 30(7-8), 363-368. doi:10.1016/j.matbio.2011.06.001
- Ketchen, S., Rohwedder, A., Knipp, S., Esteves, F., Struve, N., Peckham, M., Ladbury, J., Curd, A., Short, S., Brüning-Richardson, A. (2020). A novel workflow for three-dimensional analysis of tumour cell migration. *Interface Focus*, 10(2), doi:10.1098/rsfs.2019.0070
- Kosla, J., Paňková, D., Plachý, J., Tolde, O., Bicanová, K., Dvořák, M., Rösel, D. and Brábek, J. (2013). Metastasis of aggressive amoeboid sarcoma cells is dependent on Rho/ROCK/MLC signaling. *Cell Communication and Signaling*, 11(1), 51. doi:10.1186/1478-811X-11-51
- Maziveyi, M., Alahari, S. (2017). Cell matrix adhesions in cancer: The proteins that form the glue. *Oncotarget*, 8(29), 48471-48487. doi:10.18632/oncotarget.17265
- Parri, M., Chiarugi, P. (2010). Rac and Rho GTPases in cancer cell motility control. *Cell Communication and Signaling*, 8(1), doi:10.1186/1478-811X-8-23
- Shang, X., Marchioni, F., Sipes, N., Evelyn, C.R., Jerabek-Willemsen, M., Dühr, S., Seibel, W., Wortman, M., Zheng, Y. (2012). Rational design of small molecule inhibitors targeting RhoA subfamily Rho GTPases. *Chemistry & Biology*, 19(6), 699-710. doi:10.1016/j.jchembiol.2012.05.009
- Siegel, R., Miller, K., Jemal, A. (2018). Cancer statistics, 2018. *CA: A Cancer Journal for Clinicians*, 68(1), 7-30. doi:10.3322/caac.21442
- Sun, S., Zhang, G., Sun, Q., Wu, Z., Shi, W., Yang, B., Li, Y. (2015). Insulin-induced gene 2 expression correlates with colorectal cancer metastasis and disease outcome. *IUBMB Life*, 68(1), 65-71. doi: 10.1002/iub.1461

---

Tocris. Cat. No. 5003- Rhosin hydrochloride [Online image]. Retrieved from [https://www.tocris.com/products/rhosin-hydrochloride\\_5003](https://www.tocris.com/products/rhosin-hydrochloride_5003)

Tocris. Cat. No. 5233 - CCG 1423 [Online image]. Retrieved from [https://www.tocris.com/products/ccg-1423\\_5233](https://www.tocris.com/products/ccg-1423_5233)

Tojkander, S., Gateva, G., Lappalainen, P. (2012). Actin stress fibers - assembly, dynamics and biological roles. *Journal of Cell Science*, 125(8), 1855-1864. doi:10.1242/jcs.098087

Vallenius, T. (2013). Actin stress fibre subtypes in mesenchymal-migrating cells. *Open Biology*, 3(6), 130001. doi:10.1098/rsob.130001

Vogt, S., Grosse, R., Schultz, G., Offermanns, S. (2003). Receptor-dependent RhoA activation in G12/G13-deficient cells: genetic evidence for an involvement of Gq/G11. *The Journal of Biological Chemistry*, 278(31), 28743-28749. doi:10.1074/jbc.M304570200

Wikipedia. GPCR-Zyklus [Online image]. Retrieved from [https://en.wikipedia.org/wiki/G\\_protein](https://en.wikipedia.org/wiki/G_protein)